



Unicellular ancestry and mechanisms of diversification of Goodpasture antigen-binding protein

Received for publication, October 12, 2018 Published, Papers in Press, October 30, 2018, DOI 10.1074/jbc.RA118.006225

Carl Darris^{‡1}, Fernando Revert[§], Francisco Revert-Ros[§], Roberto Gozalbo-Rovira[§], Andrew Feigley^{‡¶}, Aaron Fidler^{¶¶}, Ernesto Lopez-Pascual[§], Juan Saus^{§||2}, and Billy G. Hudson^{‡¶***§§¶¶|||***2,3}

From the [‡]Department of Medicine/Division of Nephrology and Hypertension and Vanderbilt University Medical Center, Vanderbilt University, Nashville, Tennessee 37232, [§]Fibrostatin, SL, Scientific Park of the University of Valencia, 46980 Paterna, Valencia, Spain, the ^{||}Department of Biochemistry and Molecular Biology, Faculty of Medicine and Dentistry, University of València, 46010 Valencia, Spain, and the [¶]Aspirnaut Program, ^{**}Center for Matrix Biology, ^{‡‡}Department of Pathology, Microbiology, and Immunology, ^{§§}Department of Cell and Developmental Biology, ^{¶¶}Department of Biochemistry, ^{|||}Vanderbilt-Ingram Cancer Center, and ^{***}Vanderbilt Institute of Chemical Biology, Vanderbilt University Medical Center, Nashville, Tennessee 37232

Edited by Gerald W. Hart

The emergence of the basement membrane (BM), a specialized form of extracellular matrix, was essential in the unicellular transition to multicellularity. However, the mechanism is unknown. Goodpasture antigen-binding protein (GPBP), a BM protein, was uniquely poised to play diverse roles in this transition owing to its multiple isoforms (GPBP-1, -2, and -3) with varied intracellular and extracellular functions (ceramide trafficker and protein kinase). We sought to determine the evolutionary origin of GPBP isoforms. Our findings reveal the presence of GPBP in unicellular protists, with GPBP-2 as the most ancient isoform. In vertebrates, GPBP-1 assumed extracellular function that is further enhanced by membrane-bound GPBP-3 in mammals, whereas GPBP-2 retained intracellular function. Moreover, GPBP-2 possesses a dual intracellular/extracellular function in cnidarians, an early nonbilaterian group. We conclude that GPBP functioning both inside and outside the cell was of fundamental importance for the evolutionary transition to animal multicellularity and tissue evolution.

The emergence of multicellular metazoans from unicellular protists coincided with the appearance of a specialized form of extracellular matrix, the basement membrane (BM)⁴ (1–5). A

This work was supported by NIDDK, National Institutes of Health, Grants R01DK 28381-4651 and R01DK18381; Atracció de Talent from the University of Valencia; El Plan Nacional de Investigación Científica, Desarrollo e Innovación Grant RTC-2014-2415-1; and Conselleria de Educació e Generalitat Valenciana Grant PROMETEOII/2014/048; and The Aspirnaut Program (to Julie K. Hudson and B. G. H.). The authors declare that they have no conflicts of interest with the contents of this article. The content is solely the responsibility of the authors and does not necessarily represent the official views of the National Institutes of Health.

This article was selected as one of our Editors' Picks.

This article contains Table S1 and Figs. S1–S4.

¹ To whom correspondence may be addressed: Division of Nephrology, Vanderbilt University Medical Center, S-3223 MCN, 1161 21st Ave. South, Nashville, TN 37232-2372. E-mail: carl.darris@vanderbilt.edu.

² Co-senior authors.

³ To whom correspondence may be addressed: Vanderbilt University Medical Center, Nashville, TN 37232. E-mail: billy.hudson@vanderbilt.edu.

⁴ The abbreviations used are: BM, basement membrane; SR, serine repeat motif; GPBP, Goodpasture antigen-binding protein; MSA, multiple-sequence alignment; PH, pleckstrin homology; LS, leading sequence; ER, endoplasmic reticulum.

This is an Open Access article under the [CC BY](https://creativecommons.org/licenses/by/4.0/) license.



myriad of studies in bilaterians have revealed a multiplicity of functions of BMs in tissue development, homeostasis, and diseases (6, 7). These include compartmentalization and maintenance of tissue architecture, organizing growth factors, signaling gradients, guiding cell migration and adhesion, delineating apical-basal polarity, modulating cell differentiation during development, orchestrating cell behavior in tissue repair after injury, and guiding organ regeneration (4, 8–13). Recent developmental studies have shifted the view of BM from one of a static support structure to that of a dynamic scaffold that is regularly remodeled to actively shape tissues and direct cell behavior (5, 14–16).

Despite these advances, there is a major gap in knowledge on the composition and function of BM at the transition from unicellular protists to multicellular animals, a pivotal event in metazoan evolution. The functionality of the BM in bilaterians is conferred by a toolkit of proteins that assemble into a supra-molecular scaffold (1, 2). These proteins include collagen IV, laminin, nidogen, and agrin/perlecan (17–19). Recently, additional proteins were identified: peroxidase (20), lysyl oxidase II (21), and Goodpasture antigen-binding protein (GPBP) (22–24). Recent studies in nonbilaterian animals have shown that collagen IV and laminin (25) are the earliest components of basement membrane, as evidenced in ctenophores and sponges, the two oldest animal lineages, and were likely essential for animal multicellularity (2, 3).

Among BM proteins, GPBP was uniquely poised to also play a role in the appearance of BMs and the transition to multicellularity, owing to its multiple isoforms (23, 26, 27) with varied functions both inside (28, 29) and outside of cells (22–24, 30).

Human GPBP is encoded by the *COL4A3BP* gene and is transcribed into multiple isoforms (Fig. 1). GPBP-1 mainly functions on the outside of cell as a kinase that phosphorylates collagen IV (23) and plays a role in BM assembly (22, 24, 30). GPBP-2 (also referred to as GPBPΔ26 or CERT, ceramide transporter protein) mainly functions inside of cells translocating ceramides (26, 28). GPBP-3 is membrane-bound and functions to increase the secretion of GPBP-1 into the extracellular matrix (27). GPBP-1 and GPBP-2 are associated with a vast array of biological and pathological processes, including

The evolution and diversification of GPBP

Human Isoforms of GPBP

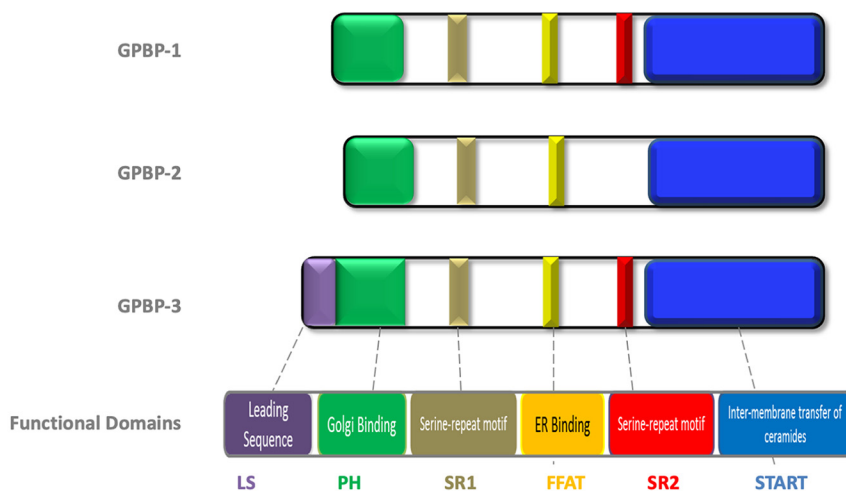


Figure 1. GPBP structure. GPBP is a multidomain protein comprising a leading sequence (LS), PH domain, SR1 and SR2 domains, a FFAT motif, and a START domain. GPBP-1 lacks the LS domain, GPBP-2 lacks the LS domain and SR2 domain, and GPBP-3 contains all domains.

muscle and brain development and differentiation (29, 31), neuronal degradation (32), oxidative stress response (33), chemotherapeutic resistance of cancer cells (24, 34), and altered collagen IV formation (24, 30). An understanding of the evolution and divergence of GPBP isoforms may shed light on the role they played in the evolutionary transition to multicellular animals.

Importantly, comparison of metazoans to unicellular relatives may shed light on the evolutionary transition to multicellularity in animals (35). Previous phylogenetic studies of GPBP-1 and GPBP-2 were based on genomic data (35–37) from bilaterian and some nonbilaterian animals. Here, we extended the phylogenetic studies to include analysis of newly available transcriptomic and genomic data from bilaterian and nonbilaterian and unicellular protists. Our findings reveal that GPBP-2 is the most ancient isoform, originating in the last common ancestor of filastereans, choanoflagellates, and metazoans. GPBP-2 having both intra- and extracellular functions in early metazoans likely played a role in the evolutionary transition to multicellular animals.

Results

Unicellular origin and evolution of GPBP

We traced the evolution of GPBP by analyzing transcriptomic data across multiple phyla. We used multiple-sequence alignments (MSAs) to characterize the six functional domains of GPBP (Fig. 1). Among these, the serine repeat motif 2 (SR2) domain is a distinguishing feature (26–28, 31). GPBP-1 and GPBP-3 both contain an SR2 domain and have extracellular related functions, whereas GPBP-2, characterized by the absence of an SR2 domain, has an intracellular function (28). GPBP isoforms containing an SR2 domain were only found in chordates, indicating that GPBP-1 and -3 are absent among invertebrate animals, choanoflagellates, and filastereans (Fig. 2A and Fig. S1). Isoforms lacking an SR2 domain were identified across all groups, indicating that GPBP-2 is conserved across animals, choanoflagellates, and filastereans (Fig. 2B and Fig. S2).

The conservation of the five other functional domains is unknown. We used MSAs to assess their phylogenetic distribution and conservation. The PH domain is an N-terminal phosphoinositide recognition domain that binds the Golgi membrane via phosphoinositide 4-monophosphate (23, 38). The COF (CERT, OSBP, and FAPP) motif (KWTNYIHGWQ) within the PH domain is essential for Golgi-specific recognition and binding (28, 39). MSA analysis reveals that the COF motif is well conserved throughout the animal kingdom. Among the representative animal species in our data set, only lamprey lacked conservation of the COF motif. Conservation of the COF motif extended to GPBP sequences from choanozoan and filasterian organisms (Figs. S1 and S2). The middle region of GPBP contains a FFAT motif, comprising two phenylalanine residues in an acid track (EFFDAXE), which interacts with the endoplasmic reticulum (ER) membrane protein vesicle-associated membrane protein-associated protein. Toward the C-terminal end of the protein, the START domain binds and transports ceramides (40). Multiple sequence alignments show strong conservation of the FFAT motif and START domain (Fig. 3 and Figs. S1 and S2). Collectively, our findings reveal that GPBP originated in the last common ancestor of metazoans, choanoflagellates, and filastereans, with GPBP-2 being the most ancient isoform (Fig. 3).

Genomic arrangement of *COL4A3BP* orthologs

Conservation of the collinear arrangement of genes (synteny) is considered a strong indication of functional conservation across species (41). Synteny analysis can be performed on a macro (genomic) or micro (genomic fragment) scale. We used microsynteny analysis to determine the presence or absence of shared synteny around *COL4A3BP* in diverse and phylogenetically relevant genomes. Human *COL4A3BP* was used as bait in genome database searches. No orthologs of *COL4A3BP* were detected in fungi or plant genomes. Orthologs of *COL4A3BP* were found in filasterian, choanozoan, and metazoan genomes.

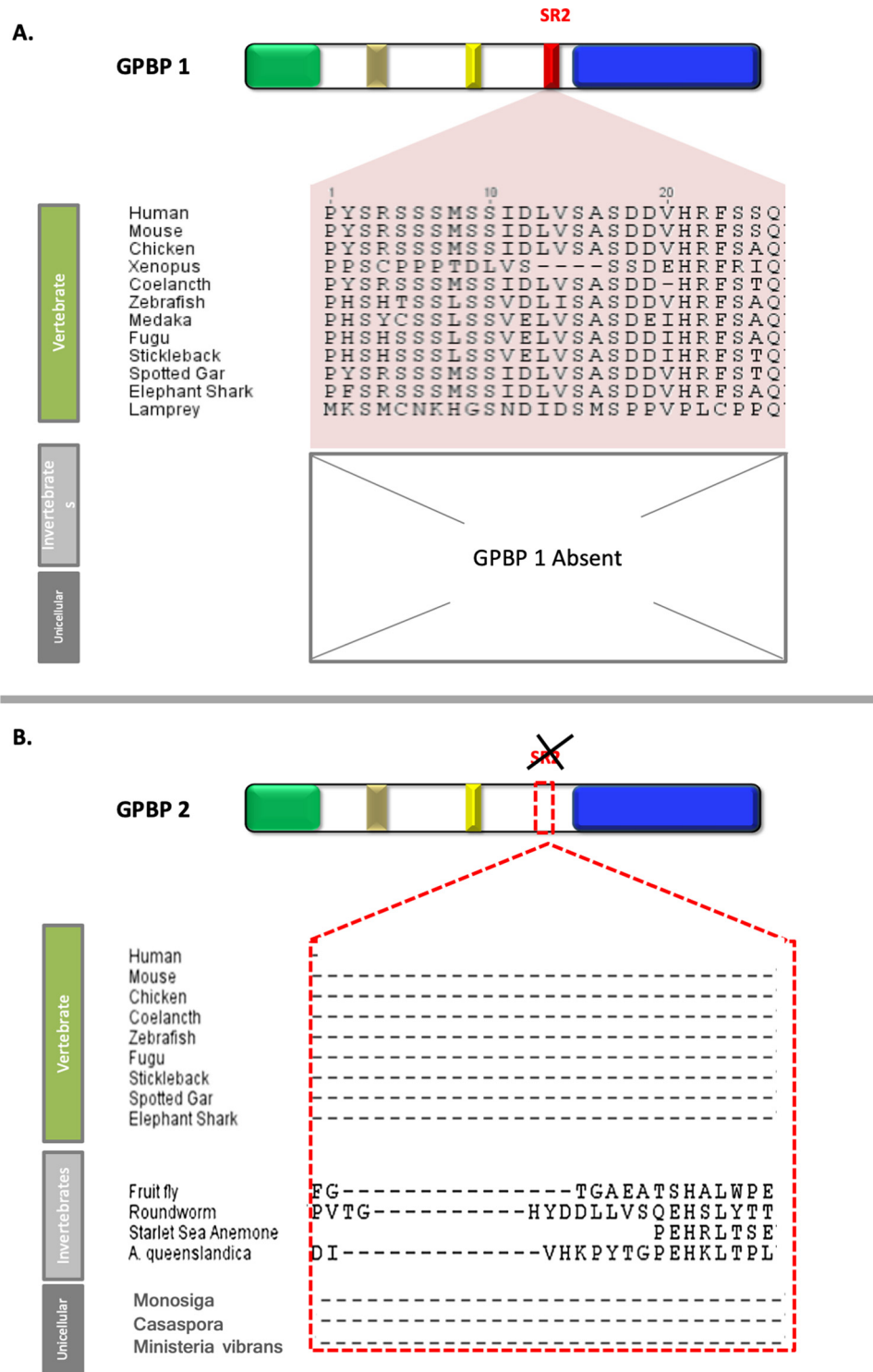


Figure 2. SR2 domain conservation emerges early in chordate evolution. Multiple-sequence alignments highlight the presence of the SR2 domain in vertebrate species (A) and its absence among invertebrate and unicellular orthologs of GPBP (B). (Information was extracted from full sequences in Figs. S1 and S2.)

Our analysis revealed that the genomes of unicellular organisms, invertebrates, and chordates each possess separate and differentiating patterns of gene clustering among genes immediately neighboring *COL4A3BP*. Analysis of vertebrate genomes revealed shared microsynteny in the genomic region containing *COL4A3BP*, DNA polymerase κ (*POLK*), 3-hydroxy-3-methylglutaryl-CoA reductase (*HMGCR*), ankyrin repeat domain 31 (*ANKRD31*),

and ankyrin repeat domain 1 (*ANKD18*) orthologs. Notably, the clustering of *COL4A3BP* and DNA polymerase κ (*POLK*) on the same chromosome is a consistent feature throughout vertebrates (Fig. 4). Previously, we have demonstrated that *POLK* and *COL4A3BP* are oriented in a head-to-head fashion and share a bidirectional promoter (42). Our current findings provide the first evidence of an evolutionary link in

The evolution and diversification of GPBP

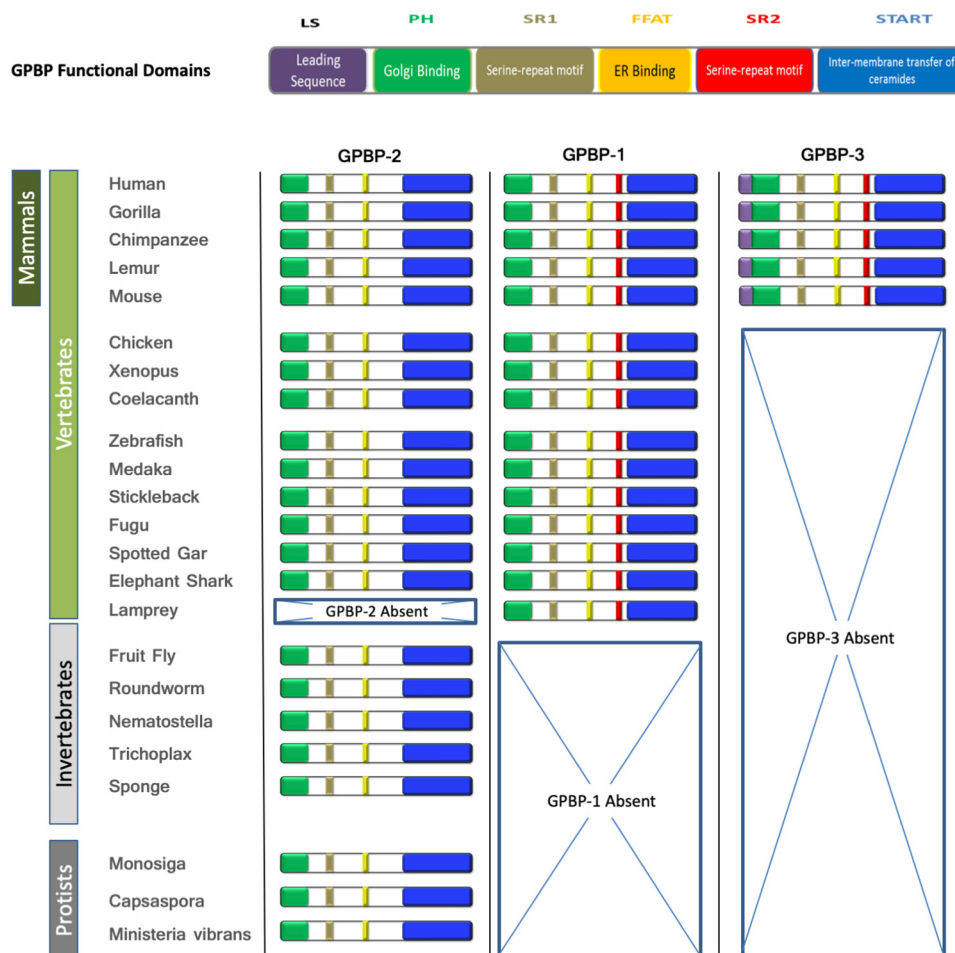


Figure 3. Phylogenetic distribution of GPBP isoforms. Transcriptomic databases were mined for the presence of GPBP isoforms in representative species across multiple phyla. GPBP-2 is the only isoform detected in unicellular protist and invertebrate organisms. GPBP-1 emerges early in vertebrate evolution. GPBP-3 occurs only in mammals.

their expression. In contrast, we found that unicellular and invertebrate genomes lack conservation of gene arrangement immediately around the *COL4A3BP* locus (Fig. 4). These findings illustrate a change in gene clustering and genomic arrangement of *COL4A3BP* at the evolutionary point of GPBP-1 emergence.

Evolution of *COL4A3BP* gene

Evolutionary changes in gene structure occur through a variety of mechanisms that can directly contribute to proteome diversity (43–45). We sought to determine the impact of evolutionary changes in *COL4A3BP* gene structure on the divergence of GPBP isoforms through comparative mapping of intronic regions and analysis of 5'-UTR sequences. Our studies revealed that modifications to *COL4A3BP* gene structure follow the same evolutionary pattern revealed in our microsynteny analysis. Among unicellular protists and invertebrate orthologs, no conservation of *COL4A3BP* gene structure was observed. Intron sequence analysis uncovered 51 unique intron sequences and 11 intron gain events throughout the evolutionary history of *COL4A3BP*. Phylogenetic mapping of intronic sequences identified three intron gain events specific to vertebrates, one of which is positioned just before the SR2-encoding exon. A second gnathostome-

specific intron was identified just after the SR2 domain-encoding exon (exon 11 in *COL4A3BP*). The conservation of these two introns is a distinguishing feature of *COL4A3BP* orthologs that encode SR2 domain-containing isoforms (GPBP-1 and GPBP-3). These findings demonstrate the mechanistic role of intron gains in the diversification of vertebrate isoforms of GPBP (Fig. 5 and Fig. S3).

Structurally, GPBP-3 is distinguished from GPBP-1 in humans by the presence of an 83-amino acid leading sequence that results from the translation of the GPBP-1 mRNA transcript at an upstream alternative non-AUG translation initiation site existing in an ORF expanding 129 residues (27). Comparative analysis of 5'-UTR sequences revealed the conservation of multiple non-AUG translation initiation sites, indicating a marsupial origin of GPBP-3 (Fig. 6).

GPBP at the dawn of multicellularity

Cnidaria is a basal phylum that is among the very first metazoans with a true basement membrane, a mesoglea that separates two cell layers. Numerous ECM components are conserved in cnidarians (46), including collagen IV, laminin, peroxidase, SPARC, and usherin. Hence, Cnidaria, such as *Nematostella vectensis* (Fig. 7), are well suited to investigate the structure, expression, and localization of GPBP-2 in tissues of a basal metazoan spe-

	Species	Chromosome	Genomic Orientation					GPBP Isoforms		
			ANKDD1B	POLK	COL4A3BP	HMGCR GCTN3	ANKRD31	GPBP-1	GPBP-2	GPBP-3
Vertebrates	Human	Chromosome 5	←	←	→	→	←	✓	✓	✓
	Mouse	Chromosome 13	←	←	→	→	←	✓	✓	✓
	Chicken	Chromosome Z	←	←	→	→	←	✓	✓	✓
	Clawed Frog	Scaffold GL172749	←	←	→	→	←	✓	✓	□
	Coelacanth	Scaffold 140	←	←	→	→	←	✓	✓	□
	Zebrafish*	Chromosome 5	←	←	→	→	←	✓	✓	□
	Medaka	Chromosome 9	←	←	→	→	←	✓	✓	□
	Pufferfish	Scaffold 4	←	←	→	→	←	✓	✓	□
	Stickleback	Group XIII	←	←	→	→	←	✓	✓	□
	Elephant Shark	Chromosome LG2	←	←	→	→	←	✓	✓	□
	Spotted Gar	Chromosome LG2	←	←	→	→	←	✓	✓	□
	Lamprey	GL476895	←	←	→	→	←	✓	□	□
Invertebrates	Fruit fly	Chromosome 3L	←	←	→	→	←	□	✓	□
	Roundworm	Chromosome 13	←	←	→	→	←	□	✓	□
	Starlet Sea Anemone	Scaffold 305	←	←	→	→	←	□	✓	□
	A. queenslandica	Contig 13522	←	←	→	→	←	□	✓	□
Unicellular	M. brevicollis	Scaffold 11	←	←	→	→	←	□	✓	□
	C. owczarzaki	Supercontig 2.11	←	←	→	→	←	□	✓	□

Figure 4. Evolutionary changes in genomic orientation of COL4A3BP. The schematic illustrates the three distinct patterns of shared synteny that delineate COL4A3BP gene family members. Chordate species have a distinguishing pattern of conserved gene arrangement around COL4A3BP, which consists of a head-to-head orientation of COL4A3BP and POLK and/or a head-to-head orientation of HMGCR and ANKDD1B. Among those Teleost species believed to have undergone 3WR, a specific pattern of shared synteny consisting of a tail-to-tail orientation of COL4A3BP and HMGCR was found, whereas invertebrate orthologs of COL4A3BP lack a distinct pattern of gene clustering. (Gene orthologs are represented by arrows of the same color; gray boxes represent nonorthologous genes). ANKDD1B, ankyrin repeat and death domain-containing 1B; ANKRD31, ankyrin repeat domain 31; COL4A3BP, collagen type IV α 3-binding protein; GCTN3, glucosaminyl (N-acetyl)transferase 4, core 2; HMGCR, 3-hydroxy-3-methylglutaryl-CoA reductase; POLK, DNA polymerase κ . Genes are illustrated in the order in which they appear on chromosomes/scaffolds for each species. Where available, the chromosome/scaffold number is provided. Gene names refer to human orthologs as listed in the Ensemble database.

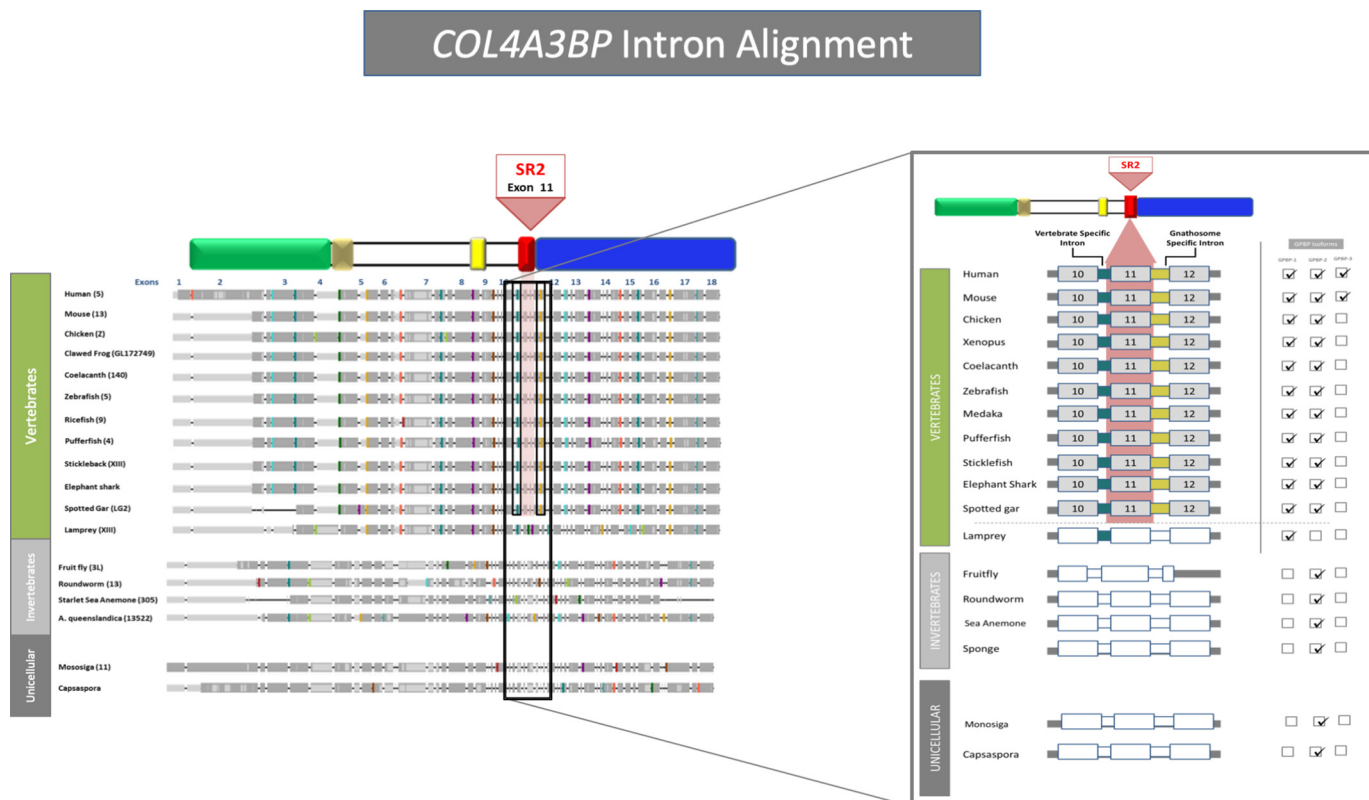


Figure 5. Genomic mechanism of GPBP isoform diversification. Alignment of conserved introns among *COL4A3BP* orthologs highlights two intron gain events specific to *COL4A3BP* orthologs that encode SR2-containing isoforms of GPBP. (See also Fig. S3.)

cies. The predicted length of *Nematostella* GPBP (NvGPBP) based on genomic data is 488 amino acids. In humans, GPBP-2 is composed of 598 amino acids. Our genomic analysis revealed several inversion errors in the GPBP coding region, which, when corrected, yielded a sequence of 615 amino acids. The expression of a single 615-amino-acid-long isoform was confirmed by transcriptome assembly and through mining of publicly available transcriptome libraries. As anticipated, NvGPBP-2 lacks an SR2 domain. NvGPBP-2 shares 65 and 50% amino acid sequence similarity with the pleckstrin homology domain and the START domain of human GPBP-2, respectively (Fig. 7B).

GPBP-2 is localized intracellularly in vertebrates; however, its localization in early metazoans is unknown. The localization of NvGPBP-2 was determined by immunohistochemical analysis using a mAb against human GPBP (N27). These analyses revealed a broad and diffuse distribution of NvGPBP-2 in both intracellular and extracellular compartments throughout the body column and tentacles (Fig. 7C). Fluorescent immunohistochemical studies reveal that NvGPBP-2 and NvCol4 co-localize at the border of the mesoglea (Fig. 7D). Additionally, studies were performed to determine whether recombinant NvGPBP-2 expressed in Sf9 insect cells was secreted or retained intracellularly. The results showed that rNvGPBP-2 was localized in both the cell pellet and the cell media (Fig. 7E), indicating both intracellular and extracellular locations. Moreover, NvGPBP-2 undergoes autophosphorylation, indicating that GPBP-2 has kinase activity, as demonstrated previously for vertebrate GPBP-2 (Fig. 7F). Together, these studies suggest that NvGPBP-2 functions both intracellularly and extracellularly

and demonstrate the early metazoan origin of GPBP-2 kinase activity.

Discussion

There is increasing evidence that the molecular machinery for regulating development, homeostasis, and immune function was present in unicellular ancestors of animals, well before the appearance of multicellularity (47–49). The identification of proteins and mechanisms co-opted during the transition to multicellular animals is essential for understanding tissue evolution, development, and disease. Emerging evidence indicates that BM, an extracellular matrix scaffold composed of numerous proteins, played an essential role in this transition. Here, we sought to determine the lineage of GPBP, a BM protein that was uniquely poised to play a role in this transition, owing to its multiple isoforms (GPBP-1, -2, and -3) with varied functions both inside and outside of cells.

Our studies reveal that GPBP-2 was the most ancient isoform, emerging over 900 million years ago in the last common ancestor of filastereans, choanoflagellates, and metazoans (Fig. S1). In vertebrates, GPBP-2, also known as CERT, mediates a nonvesicular mechanism of ceramide transport from the ER to the Golgi apparatus (28). Presumably, this intracellular CERT function is operative in the Cnidarian species and unicellular protists. Moreover, GPBP-2 may possess a second intracellular function owing to its kinase activity described for vertebrates (26) and for the Cnidarian *N. vectensis* (Fig. 7F). The detection of GPBP-2 in both compartments of the *N. vectensis* further suggests GPBP-2 functions as both an intracellular ceramide

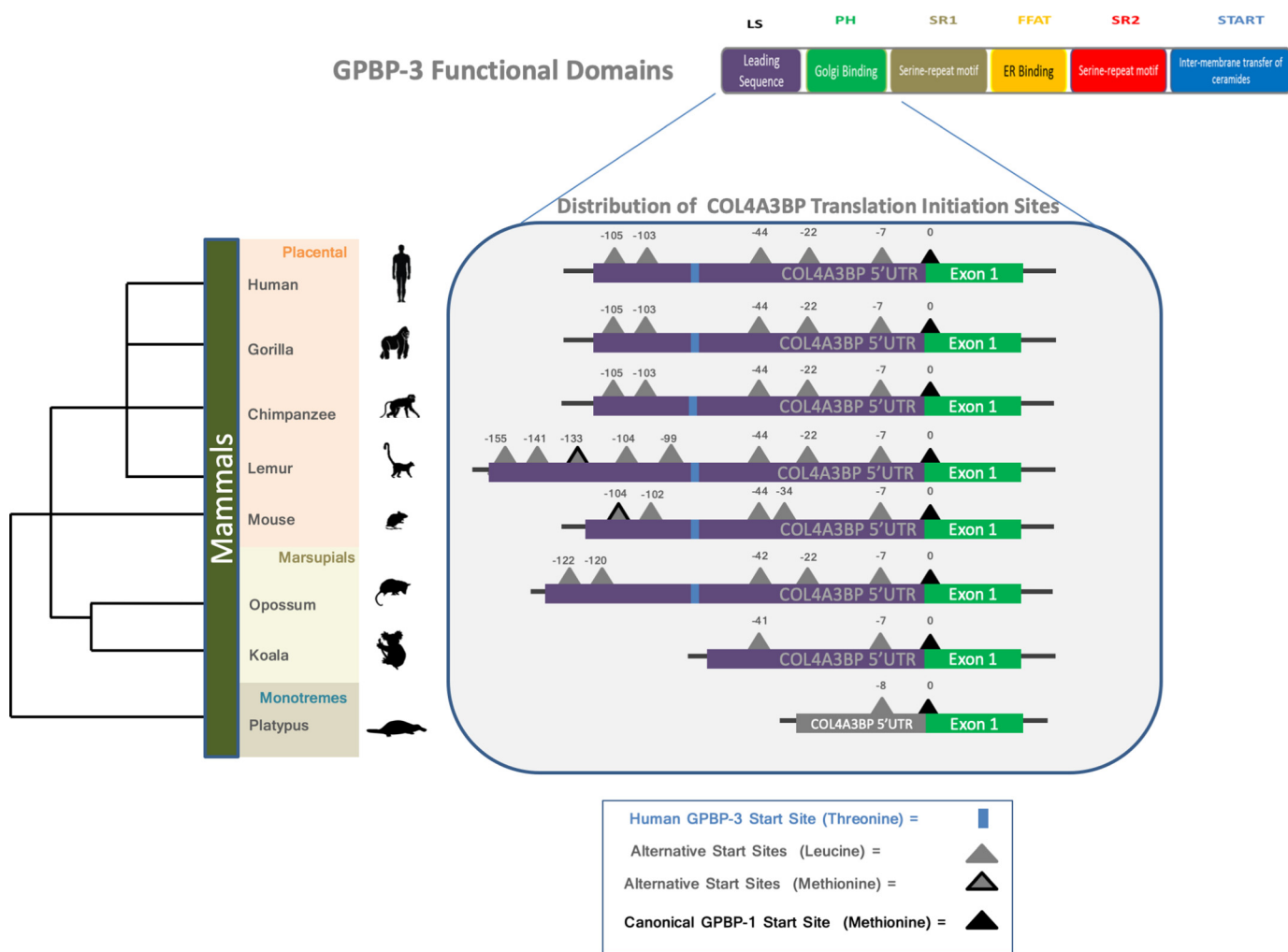


Figure 6. Conservation of COL4A3BP 5'-UTR sequences. Comparative sequence analysis reveals the marsupial origin of GPBP-3's non-AUG alternative initiation sites (gray triangles). Purple bars, 5'-UTR sequence from each organism. Canonical methionine start sites are depicted as black triangles. Negative numbers denote the position of the residue from the canonical translation initiation site. Sequences displaying conservation of the ORF sequence at their terminal end are indicated by triangles outlined in orange. (See also Fig. S4.)

transporter and an extracellular kinase. It has been demonstrated that phosphorylation of SR1 domain decreases the intracellular function of GPBP-2 (50) and protein secretion (24). Together, these studies highlight modification of the SR1 domain as a potential mechanism for toggling between the intracellular and extracellular functions of GPBP-2 in invertebrate organisms. Furthermore, GPBP-2 having both intra- and extracellular localization with the potential to function as both a lipid transporter and as a kinase in early metazoans implies that it played an important role in the evolutionary transition to multicellular animals (Fig. 8).

Our phylogenetic studies demonstrate that GPBP-1 arose as a second isoform early in chordate (Fig. 8). The emergence of GPBP-1, as an extracellular component of BM, coincided with the increased complexity of the BM that enabled the genesis and evolution of multicellular vertebrate tissues (2, 16). Key mechanisms in the diversification of GPBP-2 into GPBP-1 were intron gain events that resulted in the insertion of a second serine repeat domain (SR2). The SR2 domain of GPBP-1 is known to enhance phosphorylation potential, interaction with other basement membrane proteins, and extracellular localiza-

tion (26). These findings suggest that the enhanced extracellular kinase activity of GPBP-1 was essential for its role as an early constituent of the BM that enabled the formation and evolution of epithelial tissues. GPBP-3, a mammalian innovation (Fig. 8), further enhances GPBP-1 secretion (27). Collectively, we conclude that the GPBP isoforms, functioning both inside and outside the cell, are of fundamental importance for cell and tissue function.

Materials and methods

Conserved domain analysis

The pfam database (<http://pfam.xfam.org/>)⁵ was used to identify sequence homology and conserved domains.

Phylogenetic analysis

MSAs of GPBP proteins from various species (Table S1) were generated using Geneious software (17). Phylogenetic trees were also constructed within Geneious using RAXML (version 7.2.8)

⁵ Please note that the JBC is not responsible for the long-term archiving and maintenance of this site or any other third party hosted site.

The evolution and diversification of GPBP

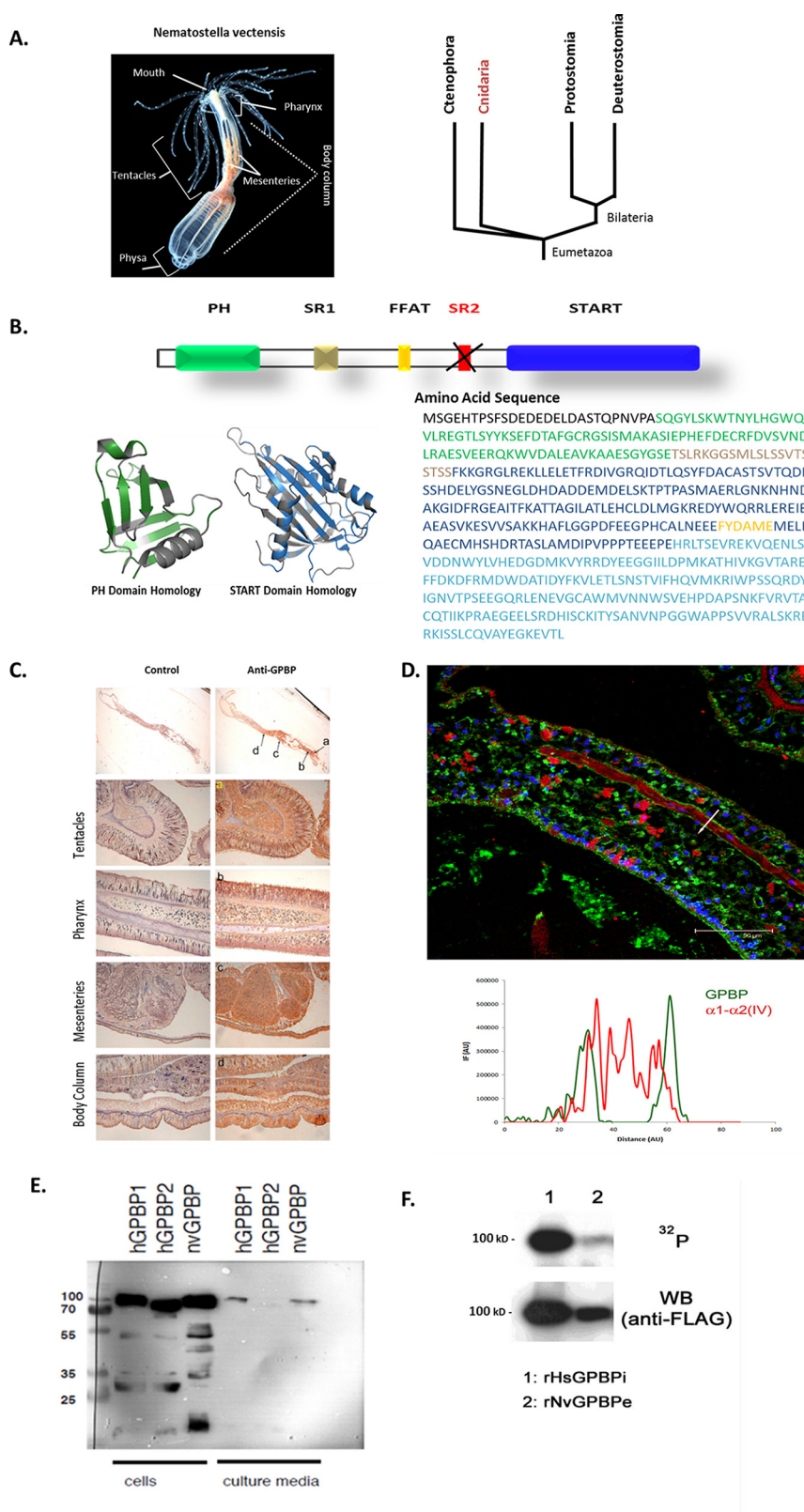


Figure 7. *Nematostella* GPBP. *A*, *Nematostella* are an anthozoan class of Cnidarians, a sister lineage to bilaterians. *B*, sequence comparison reveals 65 and 50% homology between the pleckstrin homology and the START domains of human and *Nematostella* GPBP, respectively. Correction of genomic assembly errors (underlined regions) resulted in a sequence of 615 amino acids, which lacks an SR2 domain. *C*, distribution of NvGPBP. Immunohistochemical staining of *N. vectensis* (using anti-N27) reveals a diffuse distribution of GPBP throughout the organism. *C*, NvGPBP co-localizes with collagen IV. *D*, fluorescent immunohistochemical analysis reveals the colocalization of NvGPBP and NvCOL4 throughout the mesoglea of *Nematostella vectensis*. *E*, Western blot analysis was performed for the detection of recombinant NvGPBP expressed in insect cells. Lane 1, marker; lane 2, cell lysate; lane 3, cell media. *F*, kinase assay studies demonstrate the kinase activity of GPBP-2 in *Nematostella*. Incorporation of P32 was measured using recombinant forms of human and *Nematostella* GPBP-2. A FLAG tag was incorporated in the recombinant proteins and anti-FLAG antibody was used as a loading control.

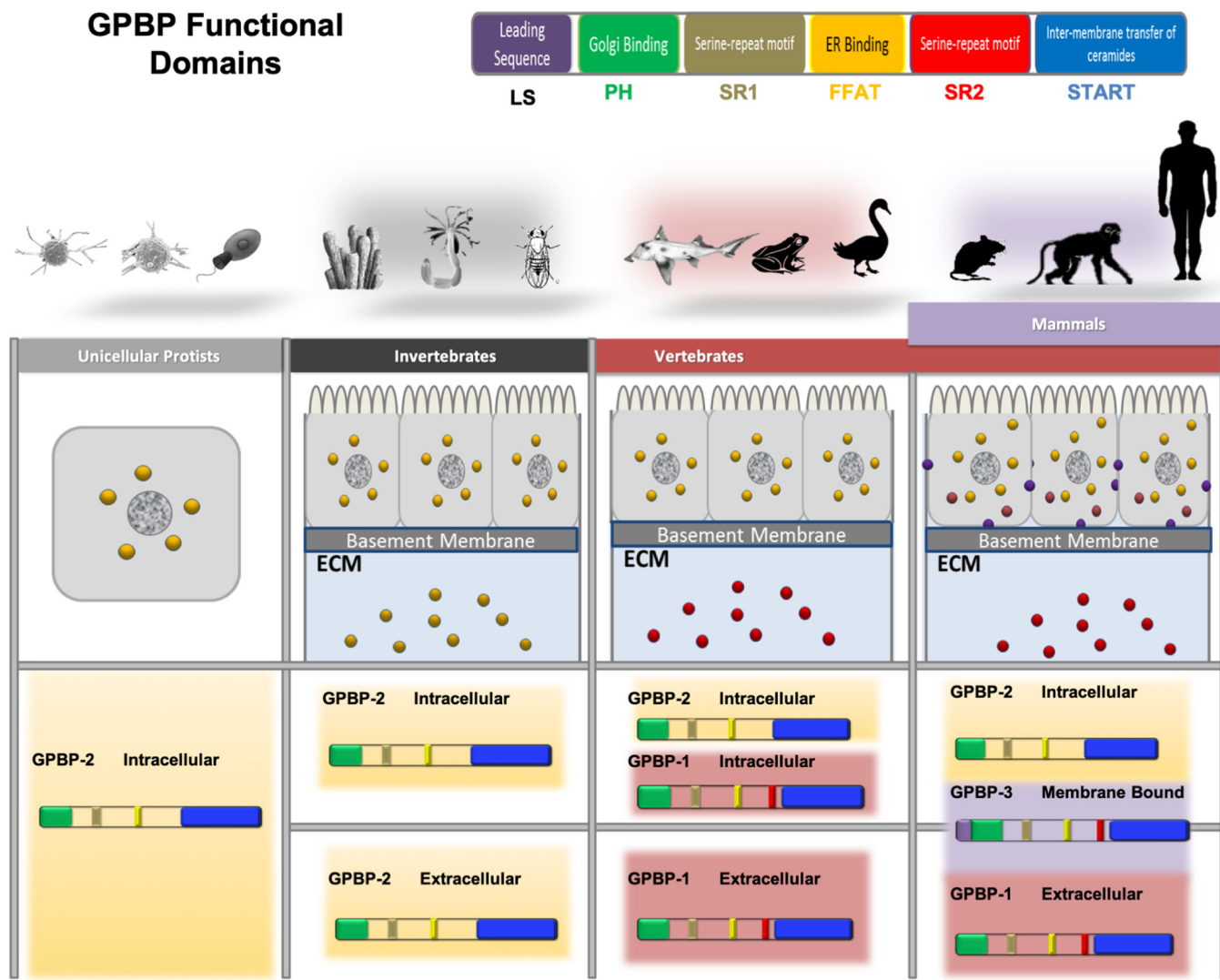


Figure 8. Schematic overview of *COL4A3BP* evolution. Three isoforms of GPBP have emerged throughout evolution. GPBP-2, the ancestral isoform of GPBP, is present in unicellular protists. Genomic rearrangements caused by intron gain events aided in the development of the SR2 domain and the emergence of GPBP-1 and GPBP-3.

with the following settings: RAXML rapid hill-climbing mode, using one distinct model/data partition with joint branch length optimization, executing 100 nonparametric bootstrap inferences, ML estimate of 25 per site rate category. Final tree likelihood was evaluated and optimized under GAMMA model parameters and estimated up to an accuracy of 0.1000000000 log likelihood units.

Identification of syntenic blocks

The conservation of gene co-localization around orthologs of *COL4A3BP* was evaluated using the UCSC genome browser (<https://genome.ucsc.edu/>),⁵ the Ensembl genome browser (<http://www.ensembl.org/>),⁵ and/or the JGI Genome Portal (<http://genome.jgi.doe.gov>).

Gene structure analysis

Cross-species analysis of *COL4A3BP* gene structure was performed using WebScipio (www.webscipio.org)⁵ (52, 53). GenePainter software was used to map gene structures, generated by WebScipio, onto protein multiple sequence align-

ments by aligning intronic regions. (The GenePainter web-server is accessible at <http://www.motorprotein.de/genepainter>)⁵ (52, 53).

Identification of non-AUG translation initiation sites

Non-AUG start sites were identified using Virtual Ribosome software (version 2) (56).

Genomic characterization of *N. vectensis* *COL4A3BP*

The genomic arrangement of *COL4A3BP* was analyzed using the *Nematostella* genome browser (<https://genome.jgi.doe.gov/Nemve1/Nemve1.home.html>) (55). Several assembly inversion errors were detected by manual inspection of the genomic region coding for NvGPBP. CLC software was used to make corrections to the genomic sequence. PCR using gap-flanking primers was used confirm sequence corrections. The following primers were used for the amplification reaction: forward, CCTGTACCACCCCTACAGA; reverse, CCC-CATCTTCATGAACCAAGT.

The evolution and diversification of GPBP

Detection of GPBP in *Nematostella*

N. vectensis homogenate samples were sonicated in lysis buffer (50 mM sodium phosphate, 2% glycerol, 0.1% Triton X-100, pH 6.5) and analyzed by SDS-PAGE. Western blotting of *N. vectensis* homogenate SDS-PAGE was performed using mouse monoclonal anti-GPBP antibody (N27-HRP) (24). Western blotting signal was developed using West Femto chemiluminescent substrate and imaged with Chemi-Doc XRS.

Expression of intracellular and extracellular NvGPBP

Flagged *Nematostella* GPBP was expressed with the Bacto-Bac[®] Baculovirus Expression System in Sf9 insect cells (Thermo Fisher Scientific).

Nematostella cDNA was amplified with primers FLAG-nvGPBP-fwd (CCGGAATTCATGGACTACAAGGACGACGA TGACAAGATGTCTGGGGAGCATACTCCGAG) and nvGPBP-rev (CTTTGTGATATTTACAGCTCGAGC-GTCACCTCTTTGCCTT), digested with the restriction enzymes EcoRI and XhoI, and subcloned into the corresponding restriction sites in pFastBac-1 (Thermo Fisher Scientific). Intracellular and extracellular proteins were obtained and purified as described previously (24).

Immunofluorescence studies

Immunofluorescence slides were prepared using both frozen and paraffin-embedded samples. *Nematostella* samples for frozen sections were prepared by immobilizing the samples in one-third strength sea salt water containing 7% MgCl₂, followed by dehydration in 10% and then 30% sucrose baths followed by flash freezing in OTC. Paraffin-embedded slides were deparaffinized and rehydrated using citrate buffer, pH 6.3. Slides were fixed with chilled acetone washed in PBS and blocked with goat serum, after which slides were treated with mouse N27 and rat JK2 mAb for 2 h and then washed in 3× PBS for 5 min. Anti-mouse or anti-rat antibody with fluorescent tag was used as secondary antibody and allowed to incubate for 1 h and 45 min and then washed with 3× PBS for 5 min. Nuclear staining was performed using 4',6-diamidino-2-phenylindole. All slides were analyzed using a high-definition microscope at the University of Valencia core. Negative controls were prepared in this manner except with the application of N27.

In vitro phosphorylation assays

Phosphorylation assays with purified recombinant *Nematostella* or human GPBP were performed as described (24).

Author contributions—C. D. and B. H. conceptualization; C. D. resources; C. D. formal analysis; C. D., F. R., F. R.-R., R. G.-R., A. Feigley, A. Fidler, and E. L.-P. investigation; C. D. visualization; C. D. methodology; C. D., J. S., and B. H. writing-original draft; C. D., J. S., and B. H. writing-review and editing; J. S. and B. H. supervision; J. S. and B. H. funding acquisition; B. H. project administration.

References

- Hynes, R. O. (2012) The evolution of metazoan extracellular matrix. *J. Cell Biol.* **196**, 671–679 [CrossRef Medline](#)
- Fidler, A. L., Darris, C. E., Chetyrkin, S. V., Pedchenko, V. K., Boudko, S. P., Brown, K. L., Gray Jerome, W., Hudson, J. K., Rokas, A., and Hudson, B. G. (2017) Collagen IV and basement membrane at the evolutionary dawn of metazoan tissues. *eLife* **6**, e24176 [CrossRef Medline](#)
- Fidler, A. L., Boudko, S. P., Rokas, A., and Hudson, B. G. (2018) The triple helix of collagens: an ancient protein structure that enabled animal multicellularity and tissue evolution. *J. Cell Sci.* **131**, jcs203950 [CrossRef Medline](#)
- Jayadev, R., and Sherwood, D. R. (2017) Basement membranes. *Curr. Biol.* **27**, R207–R211 [CrossRef Medline](#)
- Ramos-Lewis, W., and Page-McCaw, A. (2018) Basement membrane mechanics shape development: lessons from the fly. *Matrix Biol.* **10.1016/j.matbio.2018.04.004** [CrossRef Medline](#)
- Sekiguchi, R., and Yamada, K. M. (2018) Basement Membranes in Development and Disease. *Curr. Top. Dev. Biol.* **130**, 143–191 [CrossRef Medline](#)
- Iozzo, R. V., and Gubbiotti, M. A. (2018) Extracellular matrix: the driving force of mammalian diseases. *Matrix Biol.* **71**, 1–9 [Medline](#)
- Vracko, R. (1974) Basal lamina scaffold: anatomy and significance for maintenance of orderly tissue structure: a review. *Am. J. Pathol.* **77**, 314–346 [Medline](#)
- Hynes, R. O. (2009) The extracellular matrix: not just pretty fibrils. *Science* **326**, 1216–1219 [CrossRef Medline](#)
- Yurchenco, P. D. (2011) Basement membranes: cell scaffolding and signaling platforms. *Cold Spring Harb. Perspect. Biol.* **3**, a004911 [Medline](#)
- Song, J. J., and Ott, H. C. (2011) Organ engineering based on decellularized matrix scaffolds. *Trends Mol. Med.* **17**, 424–432 [CrossRef Medline](#)
- Pastor-Pareja, J. C., and Xu, T. (2011) Shaping cells and organs in *Drosophila* by opposing roles of fat body-secreted collagen IV and perlecan. *Dev. Cell* **21**, 245–256 [CrossRef Medline](#)
- Keeley, D. P., and Sherwood, D. R. (2018) Tissue linkage through adjoining basement membranes: the long and the short term of it. *Matrix Biol.* **10.1016/j.matbio.2018.05.009** [CrossRef Medline](#)
- Horne-Badovinac, S. (2014) The *Drosophila* egg chamber—a new spin on how tissues elongate. *Integr. Comp. Biol.* **54**, 667–676 [CrossRef Medline](#)
- Daley, W. P., and Yamada, K. M. (2013) ECM-modulated cellular dynamics as a driving force for tissue morphogenesis. *Curr. Opin. Genet. Dev.* **23**, 408–414 [CrossRef Medline](#)
- Morrissey, M. A., and Sherwood, D. R. (2015) An active role for basement membrane assembly and modification in tissue sculpting. *J. Cell Sci.* **128**, 1661–1668 [CrossRef Medline](#)
- Gubbiotti, M. A., Neill, T., and Iozzo, R. V. (2017) A current view of perlecan in physiology and pathology: a mosaic of functions. *Matrix Biol.* **57**, 285–298 [Medline](#)
- Pozzi, A., Yurchenco, P. D., and Iozzo, R. V. (2017) The nature and biology of basement membranes. *Matrix Biol.* **57**, 1–11 [Medline](#)
- Yurchenco, P. D. (2015) Integrating activities of laminins that drive basement membrane assembly and function. *Curr. Top. Membr.* **76**, 1–30 [CrossRef Medline](#)
- Bhave, G., Cummings, C. F., Vanacore, R. M., Kumagai-Cresse, C., Ero-Tolliver, I. A., Rafi, M., Kang, J.-S., Pedchenko, V., Fessler, L. I., Fessler, J. H., and Hudson, B. G. (2012) Peroxidase forms sulfilimine chemical bonds using hypohalous acids in tissue genesis. *Nat. Chem. Biol.* **8**, 784–790 [CrossRef Medline](#)
- López-Jiménez, A. J., Basak, T., and Vanacore, R. M. (2017) Proteolytic processing of lysyl oxidase-like-2 in the extracellular matrix is required for crosslinking of basement membrane collagen IV. *J. Biol. Chem.* **292**, 16970–16982 [CrossRef Medline](#)
- Jones-Paris, C. R., Paria, S., Berg, T., Saus, J., Bhave, G., Paria, B. C., and Hudson, B. G. (2017) Embryo implantation triggers dynamic spatiotemporal expression of the basement membrane toolkit during uterine reprogramming. *Matrix Biol.* **57**, 347–365 [Medline](#)
- Raya, A., Revert, F., Navarro, S., and Saus, J. (1999) Characterization of a novel type of serine/threonine kinase that specifically phosphorylates the human Goodpasture antigen. *J. Biol. Chem.* **274**, 12642–12649 [CrossRef Medline](#)
- Revert, F., Revert-Ros, F., Blasco, R., Artigot, A., López-Pascual, E., González-Rovira, R., Ventura, I., Gutiérrez-Carbonell, E., Roda, N., Ruiz-Sanchis, D., Forteza, J., Alcácer, J., Pérez-Sastre, A., Díaz, A., Pérez-Payá, E.,

- et al.* (2018) Selective targeting of collagen IV in the cancer cell microenvironment reduces tumor burden. *Oncotarget* **9**, 11020–11045 [Medline](#)
25. Brown, K. L., Cummings, C. F., Vanacore, R. M., and Hudson, B. G. (2017) Building collagen IV smart scaffolds on the outside of cells. *Protein Sci.* **26**, 2151–2161 [CrossRef Medline](#)
 26. Raya, A., Revert-Ros, F., Martínez-Martínez, P., Navarro, S., Rosello, E., Vieites, B., Granero, F., Forteza, J., and Saus, J. (2000) Goodpasture antigen-binding protein, the kinase that phosphorylates the Goodpasture antigen, is an alternatively spliced variant implicated in autoimmune pathogenesis. *J. Biol. Chem.* **275**, 40392–40399 [CrossRef Medline](#)
 27. Revert, F., Ventura, I., Martínez-Martínez, P., Granero-Moltó, F., Revert-Ros, F., Macías, J., and Saus, J. (2008) Goodpasture antigen-binding protein is a soluble exportable protein that interacts with Type IV collagen: identification of novel membrane-bound isoforms. *J. Biol. Chem.* **283**, 30246–30255 [CrossRef Medline](#)
 28. Hanada, K., Kumagai, K., Yasuda, S., Miura, Y., Kawano, M., Fukasawa, M., and Nishijima, M. (2003) Molecular machinery for non-vesicular trafficking of ceramide. *Nature* **426**, 803–809 [CrossRef Medline](#)
 29. Revert-Ros, F., López-Pascual, E., Granero-Moltó, F., Macías, J., Breyer, R., Zent, R., Hudson, B. G., Saadeddin, A., Revert, F., Blasco, R., Navarro, C., Burks, D., and Saus, J. (2011) Goodpasture antigen-binding protein (GPBP) directs myofibril formation: identification of intracellular downstream effector 130-kDa GPBP-interacting protein (GIP130). *J. Biol. Chem.* **286**, 35030–35043 [CrossRef Medline](#)
 30. Revert, F., Merino, R., Monteagudo, C., Macías, J., Peydró, A., Alcácer, J., Muniesa, P., Marquina, R., Blanco, M., Iglesias, M., Revert-Ros, F., Merino, J., and Saus, J. (2007) Increased Goodpasture antigen-binding protein expression induces type IV collagen disorganization and deposit of immunoglobulin A in glomerular basement membrane. *Am. J. Pathol.* **171**, 1419–1430 [CrossRef Medline](#)
 31. Granero-Moltó, F., Sarmah, S., O'Rear, L., Spagnoli, A., Abrahamson, D., Saus, J., Hudson, B. G., and Knapik, E. W. (2008) Goodpasture antigen-binding protein and its spliced variant, ceramide transfer protein, have different functions in the modulation of apoptosis during zebrafish development. *J. Biol. Chem.* **283**, 20495–20504 [CrossRef Medline](#)
 32. Mencarelli, C., Bode, G. H., Losen, M., Kulharia, M., Molenaar, P. C., Veerhuis, R., Steinbusch, H. W. M., De Baets, M. H., Nicolaes, G. A. F., and Martínez-Martínez, P. (2012) Goodpasture antigen-binding protein/ceramide transporter binds to human serum amyloid P-component and is present in brain amyloid plaques. *J. Biol. Chem.* **287**, 14897–14911 [CrossRef Medline](#)
 33. Rao, R. P., Yuan, C., Allegood, J. C., Rawat, S. S., Edwards, M. B., Wang, X., Merrill, A. H., Jr., Acharya, U., and Acharya, J. K. (2007) Ceramide transfer protein function is essential for normal oxidative stress response and lifespan. *Proc. Natl. Acad. Sci.* **104**, 11364–11369 [CrossRef Medline](#)
 34. Swanton, C., Marani, M., Pardo, O., Warne, P. H., Kelly, G., Sahai, E., Elustondo, F., Chang, J., Temple, J., Ahmed, A. A., Brenton, J. D., Downward, J., and Nicke, B. (2007) Regulators of mitotic arrest and ceramide metabolism are determinants of sensitivity to paclitaxel and other chemotherapeutic drugs. *Cancer Cell* **11**, 498–512 [CrossRef Medline](#)
 35. Sebé-Pedrós, A., Irimia, M., Del Campo, J., Parra-Acero, H., Russ, C., Nusbaum, C., Blencowe, B. J., and Ruiz-Trillo, I. (2013) Regulated aggregative multicellularity in a close unicellular relative of metazoa. *eLife* **2**, e01287 [CrossRef Medline](#)
 36. Richter, D. J., Fozzouni, P., Eisen, M. B., and King, N. (2018) The ancestral animal genetic toolkit revealed by diverse choanoflagellate transcriptomes. *eLife* **7**, e34226 [CrossRef Medline](#)
 37. Hanada, K. (2014) Co-evolution of sphingomyelin and the ceramide transport protein CERT. *Biochim. Biophys. Acta* **1841**, 704–719 [CrossRef Medline](#)
 38. Levine, T. P., and Munro, S. (2002) Targeting of Golgi-specific pleckstrin homology domains involves both PtdIns 4-kinase-dependent and -independent components. *Curr. Biol.* **12**, 695–704 [CrossRef Medline](#)
 39. Sugiki, T., Takeuchi, K., Yamaji, T., Takano, T., Tokunaga, Y., Kumagai, K., Hanada, K., Takahashi, H., and Shimada, I. (2012) Structural basis for the Golgi association by the pleckstrin homology domain of the ceramide trafficking protein (CERT). *J. Biol. Chem.* **287**, 33706–33718 [CrossRef Medline](#)
 40. Kudo, N., Kumagai, K., Tomishige, N., Yamaji, T., Wakatsuki, S., Nishijima, M., Hanada, K., and Kato, R. (2008) Structural basis for specific lipid recognition by CERT responsible for nonvesicular trafficking of ceramide. *Proc. Natl. Acad. Sci. U.S.A.* **105**, 488–493 [CrossRef Medline](#)
 41. Irimia, M., Tena, J. J., Alexis, M. S., Fernández-Miñán, A., Maeso, I., Bogdanovic, O., de la Calle Mustienes, E., Roy, S. W., Gómez-Skarmeta, J. L., and Fraser, H. B. (2012) Extensive conservation of ancient microsynteny across metazoans due to cis-regulatory constraints. *Genome Res.* **22**, 2356–2367 [CrossRef Medline](#)
 42. Granero, F., Revert, F., Revert-Ros, F., Lainez, S., Martínez-Martínez, P., and Saus, J. (2005) A human-specific TNF-responsive promoter for Goodpasture antigen-binding protein. *FEBS J.* **272**, 5291–5305 [CrossRef Medline](#)
 43. Hughes, A. L. (2005) Gene duplication and the origin of novel proteins. *Proc. Natl. Acad. Sci. U.S.A.* **102**, 8791–8792 [CrossRef Medline](#)
 44. Roth, C., Rastogi, S., Arvestad, L., Dittmar, K., Light, S., Ekman, D., and Liberles, D. A. (2007) Evolution after gene duplication: models, mechanisms, sequences, systems, and organisms. *J. Exp. Zool. B Mol. Dev. Evol.* **308**, 58–73 [CrossRef Medline](#)
 45. Curran, J., and Kolakofsky, D. (1988) Ribosomal initiation from an ACG codon in the Sendai virus P/C mRNA. *EMBO J.* **7**, 245–251 [CrossRef Medline](#)
 46. Tucker, R. P., Shibata, B., and Blankenship, T. N. (2011) Ultrastructure of the mesoglea of the sea anemone *Nematostella vectensis* (Edwardsiidae). *Invertebr. Biol.* **130**, 11–24 [CrossRef](#)
 47. Richter, D. J., and King, N. (2013) The genomic and cellular foundations of animal origins. *Annu. Rev. Genet.* **47**, 509–537 [CrossRef Medline](#)
 48. Rokas, A. (2008) The origins of multicellularity and the early history of the genetic toolkit for animal development. *Annu. Rev. Genet.* **42**, 235–251 [CrossRef Medline](#)
 49. Anderson, D. P., Whitney, D. S., Hanson-Smith, V., Woznica, A., Campodonico-Burnett, W., Volkman, B. F., King, N., Thornton, J. W., and Prehoda, K. E. (2016) Evolution of an ancient protein function involved in organized multicellularity in animals. *eLife* **5**, e10147 [CrossRef Medline](#)
 50. Sugiki, T., Egawa, D., Kumagai, K., Kojima, C., Fujiwara, T., Takeuchi, K., Shimada, I., Hanada, K., and Takahashi, H. (2018) Phosphoinositide binding by the PH domain in ceramide transfer protein (CERT) is inhibited by hyperphosphorylation of an adjacent serine-repeat motif. *J. Biol. Chem.* **293**, 11206–11217 [CrossRef Medline](#)
 51. Hatje, K., Keller, O., Hammesfahr, B., Pillmann, H., Waack, S., and Kollmar, M. (2011) Cross-species protein sequence and gene structure prediction with fine-tuned WebScipio 2.0 and Scipio. *BMC Res. Notes* **4**, 265 [CrossRef Medline](#)
 52. Odronitz, F., Pillmann, H., Keller, O., Waack, S., and Kollmar, M. (2008) WebScipio: an online tool for the determination of gene structures using protein sequences. *BMC Genomics* **9**, 422 [CrossRef Medline](#)
 53. Mühlhausen, S., Hellkamp, M., and Kollmar, M. (2015) GenePainter 2.0 resolves the taxonomic distribution of intron positions. *Bioinformatics* **31**, 1302–1304 [CrossRef Medline](#)
 54. Hammesfahr, B., Odronitz, F., Mühlhausen, S., Waack, S., and Kollmar, M. (2013) GenePainter: a fast tool for aligning gene structures of eukaryotic protein families, visualizing the alignments and mapping gene structures onto protein structures. *BMC Bioinformatics* **14**, 77 [CrossRef Medline](#)
 55. Putnam, N. H., Srivastava, M., Hellsten, U., Dirks, B., Chapman, J., Salamov, A., Terry, A., Shapiro, H., Lindquist, E., Kapitonov, V. V., Jurka, J., Genikhovich, G., Grigoriev, I. V., Lucas, S. M., Steele, R. E., *et al.* (2007) Sea anemone genome reveals ancestral eumetazoan gene repertoire and genomic organization. *Science* **317**, 86–94 [CrossRef Medline](#)
 56. Wernersson, R. (2006) Virtual ribosome—a comprehensive DNA translation tool with support for integration of sequence feature annotation. *Nucleic Acids Res.* **34**, W385–W388 [CrossRef Medline](#)